Molecular Dynamic Simulations of Montmorillonite-Organic Interactions under Varying Salinity: An Insight into Enhanced Oil Recovery.

Thomas Underwood, Valentina Erastova, Pablo Cubillas, and H. Chris Greenwell[*]

Department of Earth Sciences, Durham University, South Road, Durham DH1 3LE, U.K.

E-mail: chris.greenwell@durham.ac.uk

Abstract

Enhanced oil recovery is becoming commonplace in order to maximise recovery from oilfields. One of these methods, low-salinity enhanced oil recovery (EOR) has shown promise, however the fundamental underlying chemistry requires elucidating. Here, three mechanisms proposed to account for low-salinity enhanced oil recovery in sandstone reservoirs are investigated using molecular dynamic simulations. The mechanisms probed are electric double layer expansion, multicomponent ionic exchange and pH effects arising at clay mineral surfaces. Simulations of smectite basal planes interacting with uncharged non-polar decane, uncharged polar decanoic acid and charged Na-decanoate model compounds are used to this end. Various salt concentrations of NaCl are modelled: 0‰, 1‰, 5‰ and 35‰ to determine the role of salinity upon the three separate mechanisms. Furthermore, the initial oil/water-wetness of the clay surface is modeled. Results show that electric double layer expansion is not able to fully explain the effects of low-salinity enhanced oil recovery. The pH surrounding a clays basal plane, and hence the protonation and charge of acid molecules is determined to be one of the dominant effects driving low-salinity EOR. Further, results present that the presence of calcium cations can drastically alter the oil wettability of a clay mineral surface. Replacing all divalent cations with monovalent cations through multicomponent cation exchange dramatically increases the water wettability of a clay surface, and will increase EOR.

1 Introduction

In an age of increasing energy demand global oil resources must be utilized as efficiently as possible. Current primary and secondary oil recovery methods may leave up to 65% of the original oil in place (OOIP) within a reservoir.[1] Growth in oil demand, oil price and ageing reservoirs are but a few reasons why companies have been looking at different methods to optimize oil recovery rates within existing assets over the past few decades. Such techniques are referred to as enhanced oil recovery; these include a wide variety of processes such as steam injection, CO_2 injection, in situ combustion and chemical flooding. Since the 1990s an additional EOR method, injection of low-salinity water, has been tested in both the lab and the field, with promising results.[2] Low-salinity EOR could offer many economical benefits compared to other EOR methods as low-salinity water can be produced on-site and does not require the addition of specialty chemicals.

It has been established that the salinity and saturation of connate water,[3–5] the reservoir's initial wettability[3] along with the presence of clay minerals[6,7] and polar oil components[4] all

---

[*]To whom correspondence should be addressed

play an important role on the degree to which the injection of low-salinity water increases oil production. Moreover, the presence of clay minerals is seen to be a key requirement for low-salinity EOR to operate.[4,6–8] This is due to the role that clays play in determining the wettability state of a rock. Clay minerals and quartz grains are widely present in the pores of sandstone reservoirs, where they form surface coatings. As such, clay surfaces are thought to interact heavily with the polar components of oil.[4,9] Different types of clay are present in sandstone reservoirs, with the dominant clay minerals being kaolinite, illite, smectite, illite-smectite mixed layer clays and chlorite.[10] Kaolinite is considered as oil wetting while smectite/chlorite surfaces are water wetting.[11]

To date, studies have proposed more than 17 separate mechanisms by which low-salinity flooding can enhance oil recovery. These are explained in some detail in the recent review by Sheng (2014).[12] Nevertheless, a definitive conclusion as to which mechanism truly underpins low-salinity enhanced oil recovery has yet to be fully determined. In the present paper three of the frequently cited mechanisms are tested at the molecular level. They are: electric double layer (EDL) expansion, multi-component ionic exchange and pH level reactions.

The electric double layer is a description of the electric field surrounding a charged colloid particle, in this instance, a negatively charged clay particle within a reservoir. A widely accepted model of a colloidal EDL is the Gouy-Chapman-Stern double layer,[13] whereby a portion of the charge-balancing interlayer cations are adsorbed to the clay, in what is known as a Stern Layer, whilst the remaining cations and anions create the traditional diffuse double layer, see Figure 1.

The important relationship that dictates the depth of the EDL, and hence the electric field strength at a fixed point, can be predicted by DLVO theory.[13] According to DLVO theory, a clay's EDL expands as salinity decreases, hence any positively charged molecule bound to the clay surface will become more strongly attracted to the clay surface, whilst negatively charged molecules will become increasingly re-
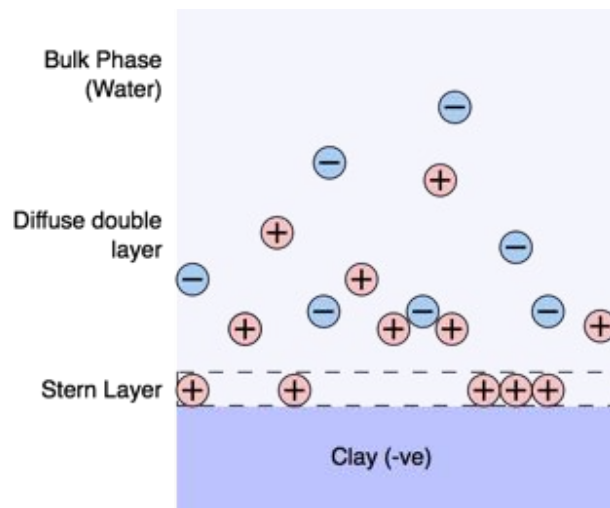

Figure 1: The Gouy-Chapman-Stern model of a clay's electric double layer.

pelled by the charged clay's surface.[13] Furthermore, as the EDL of a clay expands, it becomes more likely to interact with surrounding clay particles, and bulk clay swelling can occur. It is exactly this process that is proposed to cause the release of fine clay particles, along with associated oil, in the fines migration theory of low-salinity EOR.[4,14]

Multicomponent ionic exchange is another theory proposed to explain the effects of low-salinity EOR.[14] It is thought that there are eight separate mechanisms through which oil molecules can be bound to a clay surface,[15] though only 4 of these mechanisms are believed to be of importance to low-salinity EOR.[14] These mechanisms are presented in Table 1 and Figure 2.

Cation exchange is a mechanism whereby positively charged organics ions, such as amine/ammonium groups or heterocyclic rings containing nitrogens, are able to replace the inorganics cations that usually charge balance a clay surface (Figure 2a). Ligand bridging is a phenomenon where multivalent cations, for example Ca^{2+} or Mg^{2+}, form covalent bonds between tetrahedral clay oxygen and, for example, an oxygen atom on a charged organic molecule present in oil (Figure 2b). Cation bridging is an adsorption mechanism between organic molecules ionically bonded to divalent cations, part charge balancing the surface of the clay (Figure 2c), it is a weaker bonding

Table 1: The mechanisms of multicomponent ionic exchange.[15] Mechanisms relevant to EOR have been higlighted.[14]

Mechanism	Organic functional group
Cation exchange	Amino, ring NH, heterocyclic N (aromatic ring)
Cation bridging	Carboxylate, amines, carbonyl, alcoholic OH
Ligand exchange	Carboxylate
Water bridging	Amino, Carboxylate, carbonyl, alcoholic OH
Anion exchange	Carboxylate
Hydrogen bonding	Amino, carbonyl, carboxyl, phenolic OH
Protonation	Amino, heterocyclic N, carbonyl, carboxylate
Van der Waals interaction	Uncharged organic units

(a) Cation exchange (b) Ligand exchange (c) Cation bridging (d) Water bridging
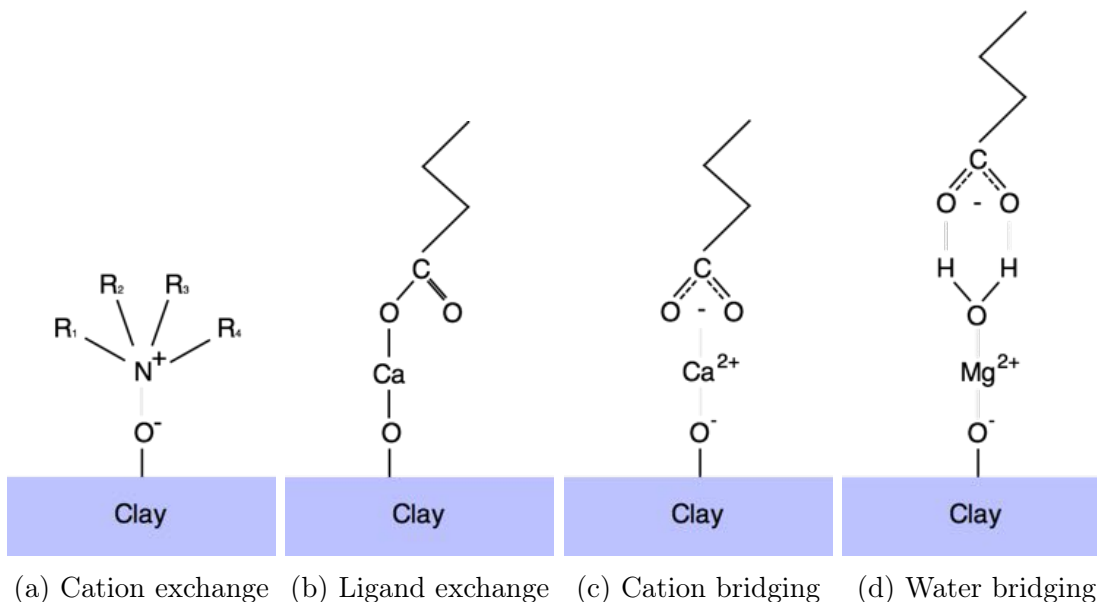
Figure 2: A schematic of the key bridging mechanisms influencing low-salinity EOR.

mechanism compared to ligand bridging. Finally, water bridging can occur if a strongly solvated cation, for example Mg^{2+}, is charge balancing the clay. In this instance, the solvation shell surrounding the Mg^{2+} ion, can order such as to attract organics through a dipole-dipole interaction (Figure 2d). It is hypothesised that low-salinity EOR occurs because the divalent cations that bridge the organic oil molecule to the clay can be readily exchanged by monovalent cations due to the expanded electric double layer,[14] thereby releasing the oil molecules through disrupting ligand bridging, cation bridging or water bridging.

To be more explicit, the mechanism leading to oil-cation-clay bridging between divalent calcium and uncharged polar organic molecule is referred to as *cation-polar bridging* in this work. The bridging mechanism via calcium ion and charged deprotonated acid is referred to as *cation-charged bridging.*

Mechanisms leading to low-salinity EOR owing to pH effects encompass a large range of effects that depend on the pH level of the system surrounding the clay surface. It has been proposed that the generation of surfactants from crude oil components at elevated (i.e. alkaline) pH levels alter the overall wettability of the reservoir matrix.[16] The concept has been further developed, with the suggestion that the injection of low-salinity water produced hydroxyl ions from a clay-calcium site, following the equilibrium reaction:[14]

$$Clay-Ca^{2+} + H_2O \rightleftharpoons Clay-H^+ + Ca^{2+} + HO^-$$
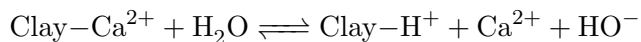
Such a pH change would cause a low-salinity flood to act like an alkaline flood, which has been theorized to improve oil recovery rates.[16] However, more recent studies dispel the hypothesis of a low-salinity flood acting akin to an alkaline flood.[14] To date, the best low-salinity water flooding results have been on crude oil that possessed an acid number less than 0.05, whilst an alkaline flood requires an acid number greater that 0.2.[14] Furthermore, it has been argued that the CO_2 found inherently within most reservoirs can act as a pH buffer in the connate water, reducing the potential of large pH fluctuations.[14]

A further pH dependent mechanism has been proposed whereby the hydroxyl ion released from a clay-calcium-water interaction is able to interact with a polar oil compound. The free hydroxyl ion interacts with a polar organic, for example a carboxylic acid, and depending on the pH level, deprotonates the organic, removing the hydrogen bonding mechanism tethering the organic to the clay.[8]

$$Clay-RCOOH + OH^- \rightleftharpoons Clay + RCOO^- + H_2O$$

A key challenge arises owing to the problems associated with probing all these postulated processes directly with molecular level insight. This is a wider challenge, occuring in related areas of clay science and to address this, computational chemistry simulations have become an essential adjunct to laboratory experimental methods for studying clay surfaces and interlayers.

In recent times, quantum mechanical (QM) simulations have become a useful tool to model the interaction of simple organic molecules on clays, for example the adsorption of monomers on kaolinite surfaces[17] amongst others.[18,19] Such methods explicitly include electron interactions, and are able to model reaction mechanisms between clay, brine, organic and water. However, the complexity of composition and structure of most clay minerals and the sheer number of interactions involved in low-salinity EOR rule out the use of QM methods with their restricted time- and length-scales in this instance.

Atomistic molecular dynamics (MD) treat atoms as spheres, intramolecularly bonded to one another via a set of springs. This simpler approach dramatically increases both the length scale and time scale that can be simulated. Indeed, classical MD is one of the key techniques used to model clay systems in the literature.[20,21] The main disadvantage of classical MD simulations is the lack of bond breaking and bond formation, hence chemical reactions are impossible to model using classical MD without specialist forcefields.[22]

The aim of the present study is to model the effects of double layer expansion, multicomponent ionic exchange, and pH levels on the absorption of organic oil molecules on smectite clay basal surfaces as a function of salt concentration using atomistic MD. This present study only considers clay basal surfaces, owing to the challenge in modeling highly dynamic and pH responsive clay edges using classical MD. Clay minerals representative in terms of structure, composition and charge density, of smectite (montmorillonite) clay basal surfaces in sandstone oil reservoirs were modelled. The effect of changing from monovalent to divalent cation type, using Na^+ and Ca^{2+}, and varying salinities from freshwater (0‰, 0 parts NaCl per 1000 H_2O by weight) to seawater (35‰) on the adhesion of model oil molecules (including non polar, polar neutral and polar charged functional groups) to clay surfaces was studied. Both initially water-wet and initially oil-wet systems have been modelled.

2 Methodology

2.1 Model Construction

The clay unit cell used in this study was a Wyoming-like montmorillonite with stoichiometry $[Al_3Mg_1] [Si_8O_{20}] (OH)_4 \cdot nH_2O$. The octahedral layer of the clay contained one Mg atom for every 3 Al atoms, whilst both tetrahedral layers contained no isomorphic substitutions. The resulting unit cell, shown in Figure 3, possessed a single net negative charge, which was subsequently balanced with intercalated Na^+ or Ca^{2+} cations in the simulations
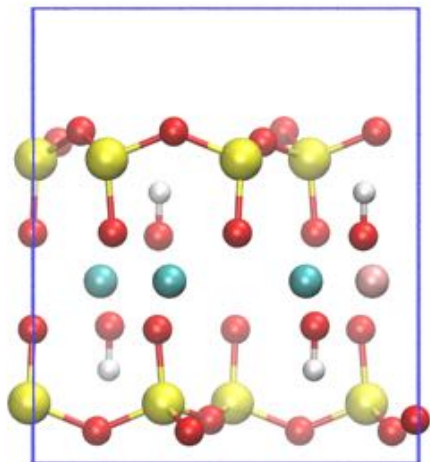
Figure 3: The montmorillonite unit cell used in this study. Colors as defined in section 2.5.

of Na-montmorillonite and Ca-montmorillonite respectively.

Montmorillonite was deemed the most suitable 2:1 clay for this study due to its high cation exchange capacity and its proposed role in low-salinity enhanced oil recovery.[10] In contrast, other clays commonly found in reservoirs, such as illites and kaolinites, possess a lower CEC or are 1:1 non-swelling clays respectively, and do not exemplify properties such as cation exchange or double layer expansion. The montmorillonite clay was constructed using data readily available on the American mineralogist crystal structure database.[23]

The organic molecules considered in this study were neutral non-polar decane ($C_{10}H_{22}$), protonated polar neutral decanoic acid ($CH_3(CH_2)_8COOH$) and charged sodium decanoate $Na^+(CH_3(CH_2)_8COO)^-$. This set of organics was ideal to highlight the effects of ionic exchange in low-salinity EOR. Additionally, pH level effects were modelled by altering the protonation state of the decanoic acid. Basal {001} surfaces of montmorillonite (the periodic models have no edge sites) are relatively pH stable and unlikely to vary within the pH range encountered within a typical oil reservoir.[24,25] All organic molecules used in this study were created using the Avogadro molecular editing suite.[26]

Periodically replicated supercells contained one layer of montmorillonite composed of 84 unit cells (12 x 7 x 1), dimensions of approximately 6 x 6 x 6 nm, and a d-spacing of approximately 5 nm. Montmorillonite structures initially occupied the region $0 < z < 0.7$ nm in all models, and the clay position varied little over all timescales modelled. Subsequently, 80 organic molecules of either decane, decanoic acid or (Na)decanoate were inserted above the single clay layer. The simulations of protonated decanoic acid represented a pH level below the pKa of decanoic acid (4.9)[27] and were ideal to probe cation-polar bridging effects. Simulations of deprotonated decanoate represented pH levels greater than the pKa of decanoic acid and were ideal to simulate the cation-charged bridging mechanism.

Initially water-wet simulations were generated by randomly dispersing the organic molecules and ions within the interlayer and subsequently solvating the system. To create initially oil-wet conditions, the clay mineral was fixed in place. The interlayer was randomly dispersed with organics and ions, and a subsequent MD simulation was run to allow the organic molecules to equilibrate at the clay surface. The system was subsequently solvated, and the position restraints on the clay layers relaxed. This process created ideal starting configurations for both water-wet and oil-wet clay surfaces, see Figures 4a and 4b respectively.

The variations of initial configurations are presented in Table 2. In total, 56 separate configurations were set up and simulated.

2.2 Parameters

The ClayFF forcefield, specifically parameterized to model clays and clay-like minerals, was used to model the montmorillonite clay within this study.[28] The ClayFF force field is designed such that the entire interactions within, and structure of, the clay is described wholly by the non-bonded Lennard-Jones and Coulomb potentials (with the exception of hydroxyl groups within the clay layer, however all hydrogen bonds were constrained in this study).

The CHARMM36 forcefield was utilized to

5

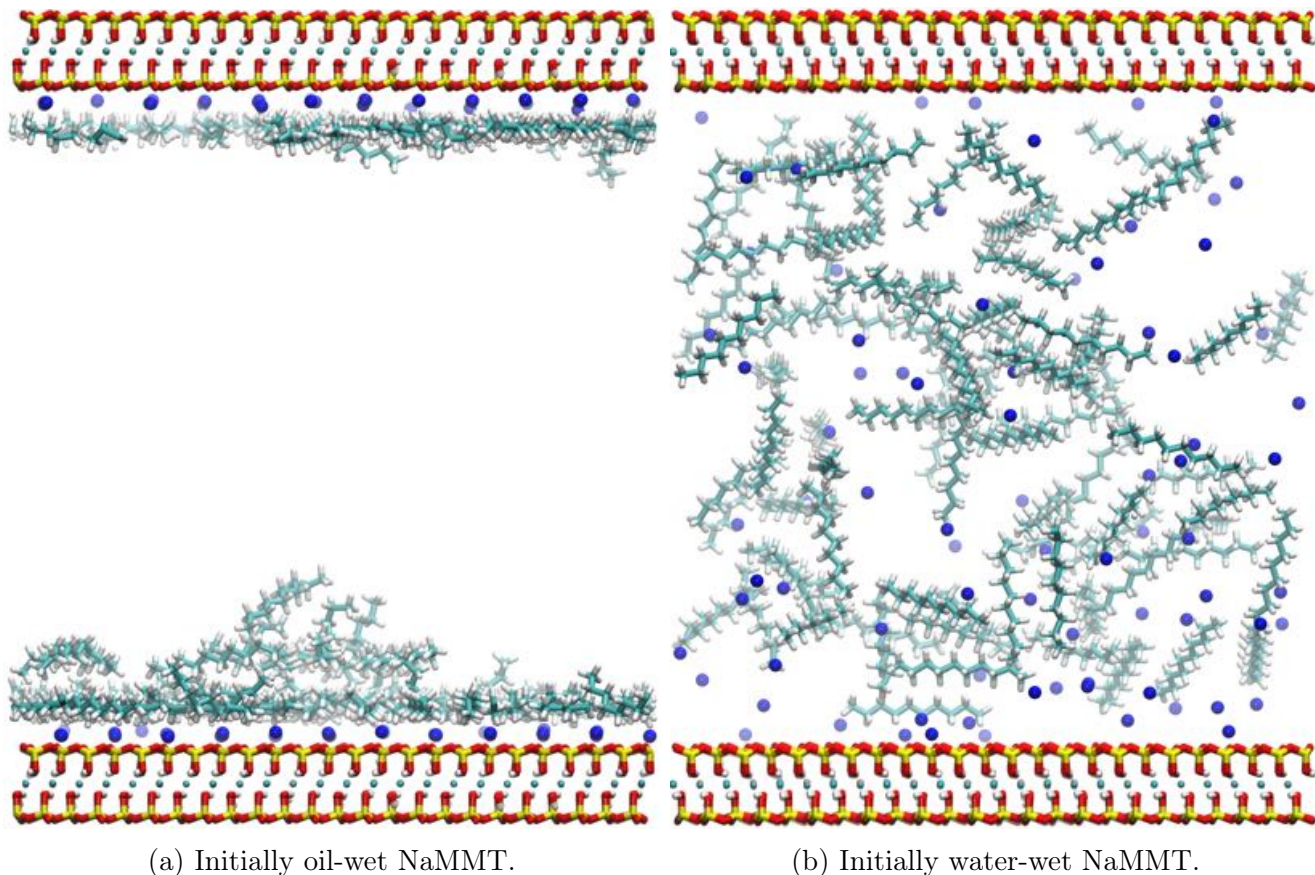(a) Initially oil-wet NaMMT.   (b) Initially water-wet NaMMT.

Figure 4: Snapshot of an initially oil-wet (left) and initially water-wet (right) NaMMT intercalated with decane molecules, pre-production, water molecules not represented. Colors as defined in section 2.5.

Table 2: The permutations of the initial conditions modelled within this study.

Variable	Permutations			
Clay Mineral	NaMMT	CaMMT		
Intercalated Organic	Decane	Decanoic Acid	Sodium Decanoate	None
Starting configuration	Oil-wet	Water-wet		
Salt concentration (NaCl)	0‰	1‰	5‰	35‰

model the organic molecules interacting with clay layers. This forcefield has been parameterized for organic systems, has proven to reproduce physically accurate representations of hydrocarbons and similar organics,[29,30] and is compatible with ClayFF.[31]

The TIP3P water model was used to simulate the water between clay layers. It has been shown that this water model is consistent with both ClayFF and CHARMM36 force fields.[31]

Lorentz-Berthelot mixing rules for van der Waals interactions are utilised in both CHARMM36 and ClayFF force fields, and have been used here to model organic-brine-clay interactions.

2.3 Simulation Details

All MD simulations were performed using GROMACS version 4.6.5[32] with electrostatic and the van der Waals cutoff distances set to 1.2 nm.

Every simulation was initialized with an energy minimization run to reduce excessive forces

on any one atom. This was accomplished using a steepest descents algorithm, with convergence achieved once the maximum force on any one atom was less than 100 kJ mol^{-1} nm^{-1}.

Subsequently, simulations were run for a 50 ps equilibration period in the constant number of particles, pressure and temperature (NPT) ensemble with a velocity-rescale Berendsen thermostat, temperature coupling constant set to 0.1 ps, and a semi-isotropic Berendsen barostat, with pressure-coupling constant 1 ps. The Berensden thermostat and barostat offered swift equilibration of the system, and convergence was validated as the d-spacing and potential energy converged.

Unless otherwise stated, equilibration was followed by a 10 ns production run in the NPT ensemble using a velocity-rescale thermostat, with a temperature coupling constant of 1 ps, and a semi-isotropic Parrinello-Rahman barostat, with a pressure coupling constant of 1 ps. All simulations were run at approximately ambient conditions, a pressure of 1 bar and a temperature of 300 K. It was necessary to run simulations at ambient, rather than reservoir temperatures, as the ClayFF force field has been parameterized to model systems at room temperature, and considerable validation would be needed against, for example neutron scattering data, to ensure it holds at high T and P, work presently ongoing for future studies.

2.4 Analysis Techniques

Analysis of densities and electric potentials across the interlayer of the clay were carried out using the analysis tools within GROMACS 4.6.5. Cluster analysis was carried out using VMD 1.9.1, with a cluster defined when two organic molecules are within 3 Å of one other, or when an organic molecule is within 3 Å of previously defined cluster. The cutoff distance was set to 3 Å to exclude water molecules being between two organics within any cluster.[33]

Divalent cation bridges were defined as any divalent cation, i.e. Ca^{2+}, within 5 Å of the clay basal plane and within 3 Å of an organic molecule. The 5 Å cutoff between clay and cation was determined using radial distribution functions (RDFs) to include the cations contained within the both the Stern layer and first hydration layer of the clay surface. Again, the 3 Å cutoff was determined to be the correct length to exclude water molecules existing between organic and divalent cation.

2.5 Visualization

All snapshots were taken using VMD 1.9.1.[34] All simulations contain a single clay layer, which has been reproduced twice in all snapshots at the bottom and top of the figures. The clay layers are identical and are periodic images of one another. The color scheme of all snapshots are defined as follows. The clay structure contains silicon (yellow), oxygen (red), aluminum (blue), magnesium (pink) and hydrogen (white) atoms. Organic molecules contain carbon (light blue), hydrogen (white) and oxygen (red). Ions are represented as large spheres and consist of sodium (blue), chlorine (red) and calcium (green) atoms. Unless specified this color scheme is kept consistent.

Density profiles between clay layers contain organics (black), sodium (blue), calcium (green) and chlorine (red).

Color schemes are presented in legends for all figures for both dynamic cluster analysis and cation bridging plots.

3 Results and Discussion

Unless otherwise stated, all data presented in the following sections were averaged from the last 5 ns of the 10 ns production simulation.

Section 3.1 discusses the potential role of double layer expansion in low-salinity EOR via MD simulations of charged smectite clays. Sections 3.2, 3.3 and 3.4 introduce organic oil molecules and examine their interactions with water-wet clay surfaces. Section 3.2 discusses non-polar uncharged decane, section 3.3 regards polar uncharged decanoic acid and section 3.4 regards the interactions of charged Na-decanoate with water-wet Na/CaMMT.

Section 3.5 discusses the key differences between initially oil-wet and water-wet simula-

tions of Na/CaMMT interacting with the complete set of oil organic molecules. Section 3.6 investigates the properties of organic desorption from CaMMT over extended production runs up to 100 ns. Sections 3.7 and 3.8 regard the dynamic properties of all simulations. Section 3.7 presents the rate of organic clustering and section 3.8 presents the rate of change of divalent cation bridges in the system as a function of time and salt concentration.

3.1 Double Layer Effects

To examine the effects of salinity on double layer expansion simulations were run on NaMMT and CaMMT without organic molecules at various brine strengths.

Figure 5a presents the electric field between the surface of the clay and $z = 2$ nm averaged over the last 5 ns of a 10 ns production run as a function of salt concentration. Figure 5b presents the electric field between the surface of the clay and $z = 2$ nm for CaMMT as a function of salt concentration. Note that the electric field strength presents identical trends for both NaMMT and CaMMT in Figure 5. This suggests that EDL expansion is not the key mechanism driving divalent cation exchange, as double layers should differ between NaMMT and CaMMT for ionic exchange to occur. Furthermore, both figures highlight several other important features.

Firstly, it can be noted that the electric field generated by the clay is entirely nulled by the charge of the ions in the double layer within 1.5 nm from the clay basal plane for both NaMMT and CaMMT at all salt concentrations. Henceforth, the results presented in subsequent sections are to be considered as simulations of organic oil molecules interacting with two independent clay basal planes, rather that organics *intercalated* between two clay sheets.

Secondly, and more pertinently, there is no correlation between double layer expansion and salt concentration present in these simulations. The results show no expansion of the EDL. The results agree with several recent findings, whereby a Stern layer of fixed cations charge balance the clay, and the simulations refute the double layer expansion hypothesis of low-salinity EOR in this instance.[35,36]

DLVO theory states that for a sufficiently highly charged clay-like surface, a Stern layer of immobile cations will be adsorbed to the clay, and act as a buffer to cancel the charge of the clay. The oscillatory nature of the electric field presented in Figure 5 can be described in this manner, whereby an immobile layer of cations charge balanced the clay, followed sequentially by a mobile layer of anions and cations.

3.2 Effect of salinity on decane

The non-polar decane models in this study include partial charges on all carbons and hydrogens atoms and are expected to scarcely interact with the clay. Previous work has shown that decane molecules form organic aggregates in brines of various strength.[37]

### 3.2.1 The interactions of decane with initially water-wet NaMMT

Figure 6a presents the final snapshot of a NaMMT simulation interacting with 80 decane molecules at a salt concentration of 5‰ NaCl.

The formation of organic aggregates is clear in Figure 6a. The decane molecules coalesce together and act independently of the charged clay surface. This behaviour is not surprising, it is energetically favourable for the hydrophobic hydrocarbons to aggregate and minimise their surface interactions with the polar solvent molecules.

Figure 7a presents the density profile of decane molecules and salt ions across the clay interlayer at varying salt concentrations. Note the symmetry across the interlayer and the discrete separation between the organic molecules and the fully-solvated ions shielding the clay. The organic molecules always form aggregates between the clay layers independent of salinity. The results show that non-polar uncharged molecules do not interact with the silicate surfaces of the water-wet clay, in concordance with previous experimental work, where the majority of hydrocarbon-clay interactions occur on hydroxyl clay surfaces.[11]
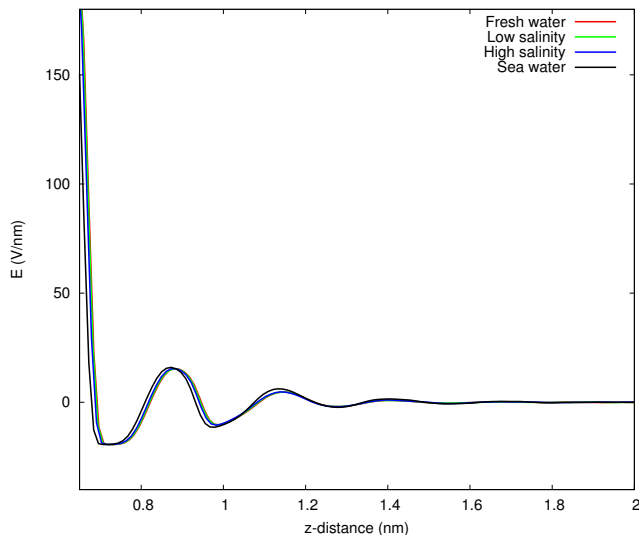
(a) The electric field strength of Na-MMT.
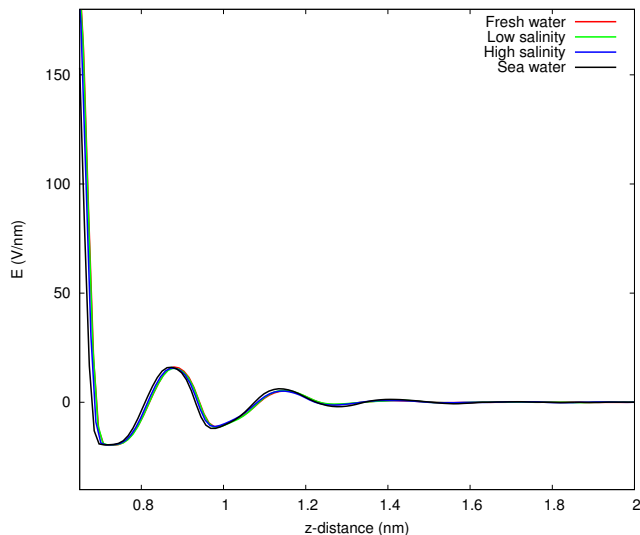
(b) The electric field strength of Ca-MMT.

Figure 5: The variation in electric field strength, and hence electric double layers, generated by NaMMT (left) and CaMMT (right) basal planes at various salinities. Colors as defined in legend.

3.2.2 The interactions of decane with initially water-wet CaMMT

The introduction of calcium as the charge balancing cation of the clay does not affect the observed behaviour of intercalated decane, see the density profile of CaMMT with decane, Figure 7b. The formation of organic aggregates can be seen across all simulations of decane, under all variations of brine strength and clay composition.

It is notable however, that the divalent calcium cations are able to form a Stern layer at the clay surface, whilst the sodium cations are always fully hydrated, as can be seen from the small peak of calcium ions adjacent to the clay in Figure 7b. A Stern layer of calcium ions was observed to form at all salt concentrations, and suggests that the divalent cation bridging mechanisms may act, at least partially, independent of the salt concentration. The results agree with the conclusions of Bourg et al, that Stern layer adsorption is independent of salinity, however, the cited study found a preference for sodium ions over calcium ions within the Stern layer.[35]

3.3 Effects of salinity on decanoic acid

The introduction of polar carboxylic functional groups in the form of decanoic acid molecules is expected to alter the behaviour of the clay-organic interactions. Bulk decanoic acid in brine forms micelles,[37] however cation-polar bridging events are expected to be seen in the simulations of decanoic acid interacting with smectite clays.

3.3.1 The interactions of decanoic acid with initially water-wet NaMMT

Figure 6b presents the final snapshot of polar uncharged decanoic acid in NaMMT with a brine concentration of 5‰ NaCl. The Figure shows that the polar uncharged organic molecules form micelles between the clay layers, with the hydrophilic carboxylic functional groups orientated on the external surface of the micelle and the hydrophobic carbohydrate tails minimising their contact with the polar water molecules on the inside of the micelle. Once again, the results show that the organic aggregates, in this case micelles, do not interact with the clay.

9
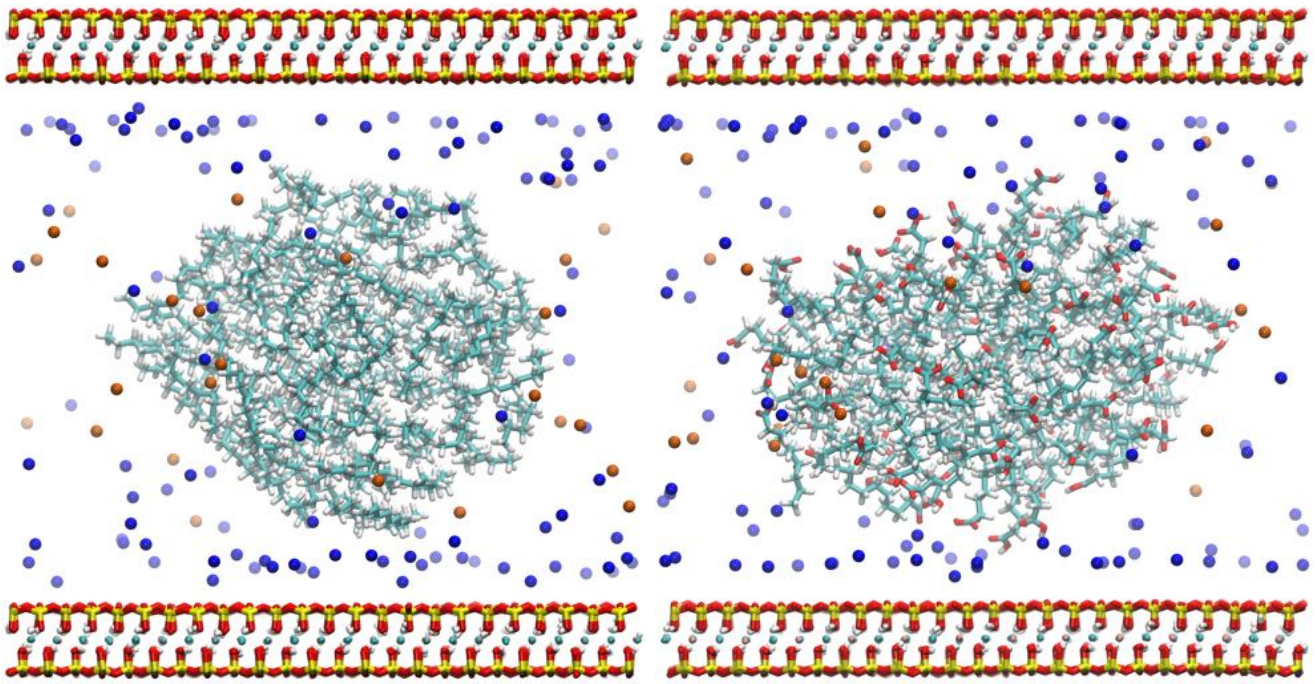
(a) A snapshot of NaMMT interacting with decane molecules.

(b) A snapshot of NaMMT interacting with decanoic acid molecules.

Figure 6: Post-production snapshots of decane (left) and decanoic acid (right) interacting with NaMMT modelled with 5‰ NaCl after 10 ns. Both snapshots present to formation of organic aggregates. Colors as defined in section 2.5.
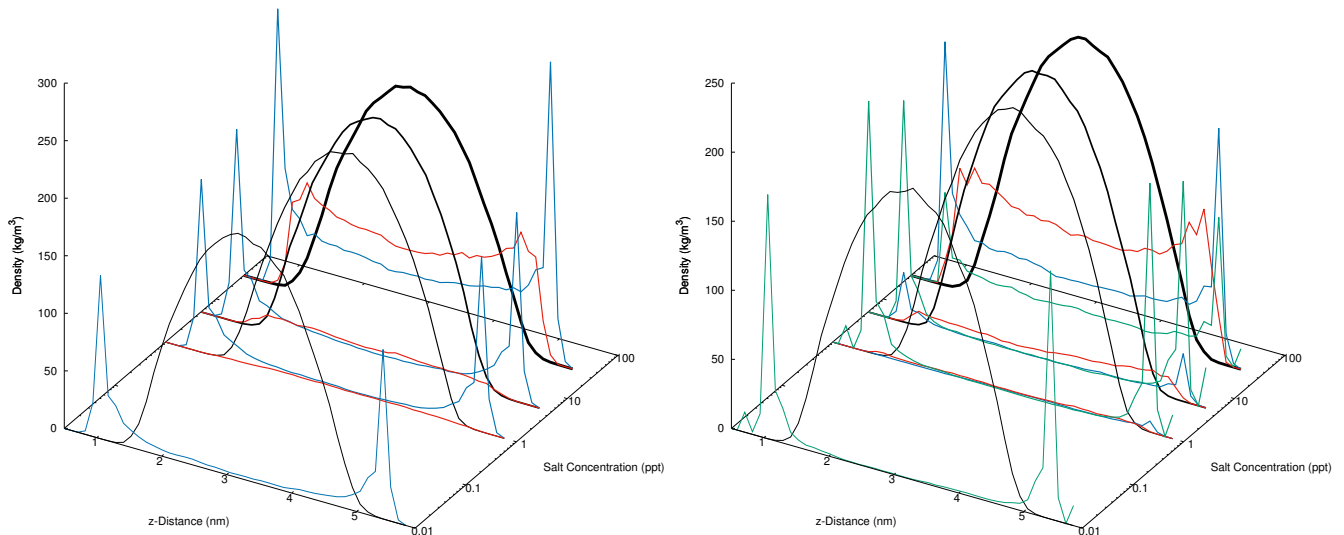
(a) The density profile of NaMMT interacting with decane.

(b) The density profile of CaMMT interacting with decane.

Figure 7: Density profiles of NaMMT (left) and CaMMT (right) interacting with decane at various salinities averaged over the last 5 ns of a 10 ns production simulation. Colors as defined in section 2.5.

3.3.2 The interactions of decanoic acid with initially water-wet CaMMT

The introduction of calcium as the charge balancing cation of the clay does not affect the observed behaviour of decanoic acid interacting with water-wet montmorillonite. The formation of micelles is observed in all simulations of decanoic acid, under all variations of brine strength and clay composition.

To summarise, the results present the formation of micelles in the simulations of polar decanoic acid interacting with both water-wet NaMMT and water-wet CaMMT at all salinities. For full listings of density profiles, see supplementary information. Furthermore, simulations show a tendency for divalent calcium cations to balance the charge of the clay and form a Stern layer. This behaviour was observed in all simulations of decane and decanoic acid interacting with water-wet CaMMT, and the behaviour is independent of salinity. The results show that cation bridging between clay and polar organic is not present in water-wet clays. The importance of initially oil-wet clays is paramount for the low-salinity EOR effect, as has been observed previously in experiments.[3]

3.4 Effects of salinity on Na-decanoate

The introduction of charged organic decanoate molecules was expected to produce the most relevant results to describe cation-charged bridging in low-salinity EOR. Interplay between clays and the organic molecules were expected to increase, as direct Coulomb forces are much stronger than the dipole interactions between polar organics.

3.4.1 The interactions of Na-Decanoate with initially water-wet NaMMT

Figure 8a is an end-snapshot of a simulation of NaMMT with 80 Na-decanoates at a salt concentration of 5‰ NaCl.

Again, the aggregation of organic molecules can be noted. The conglomerates are smaller in comparison to the uncharged polar decanoic acid molecules.

Furthermore, the distance between clay basal plane and organic cluster is larger than that in the previous examples of decane and decanoic acid. This is due to the overwhelming interaction between clay and organic being Coulomb repulsive and the absence of mediating divalent cations.

3.4.2 The interactions of Na-Decanoate with initially water-wet CaMMT

The presence of divalent calcium cations introduced several interesting features to the simulations. Figure 8b is an end-snapshot of a simulation of CaMMT interacting with 80 Na-decanoate molecules at a salt concentration of 5‰ NaCl. It can be observed that the majority of sodium and calcium cations appear to screen the charge of the clay from the organic molecules.

Despite this shielding, there are features indicative of cation-charged bridging present in figure 8b. First, note the bridging between the clay and organic molecules. See figure 9a for magnified view.

The results show the capability for divalent cations to bridge between like-charged clay layers and organic molecules. This is evidence that cation-charged bridging can play a role in oil recovery. However, the distribution of calcium cations between clay layers does not fluctuate as a function of salinity, see Figure 10. Salinity does not affect the amount of divalent cations between water-wet clays and charged organics. Hence, the cation-charged exchange mechanism is independent of salinity for water-wet clays.

Figure 8b also presents divalent cation-charged bridging between organic molecules (see 9b for an enhanced snapshot). This indicates that divalent cations within the interlayer can link separate aggregates or micelles to one another.

The density profiles present that the cation-charged bridging mechanism for charged organics is independent of salinity for water-wet clays. The snapshots show that cation-charged bridging mechanism events can occur in the simulations, however scarcely.
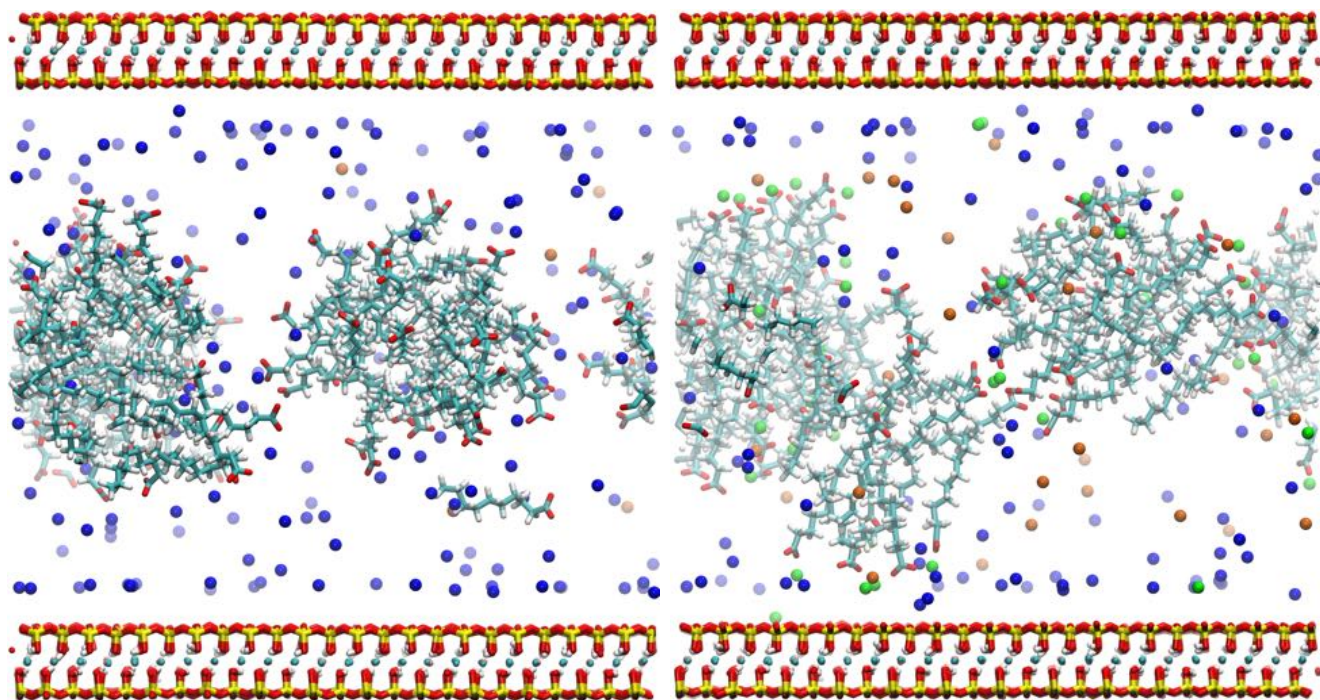
(a) A snapshot of NaMMT with 80 Na-decanoate molecules.

(b) A snapshot of CaMMT with 80 Na-decanoate molecules.

Figure 8: Post-preduction snapshots of Na-decanoate interacting with NaMMT (left) and CaMMT (right) modelled with 5‰ NaCl after 10 ns. Colors as defined in section 2.5.
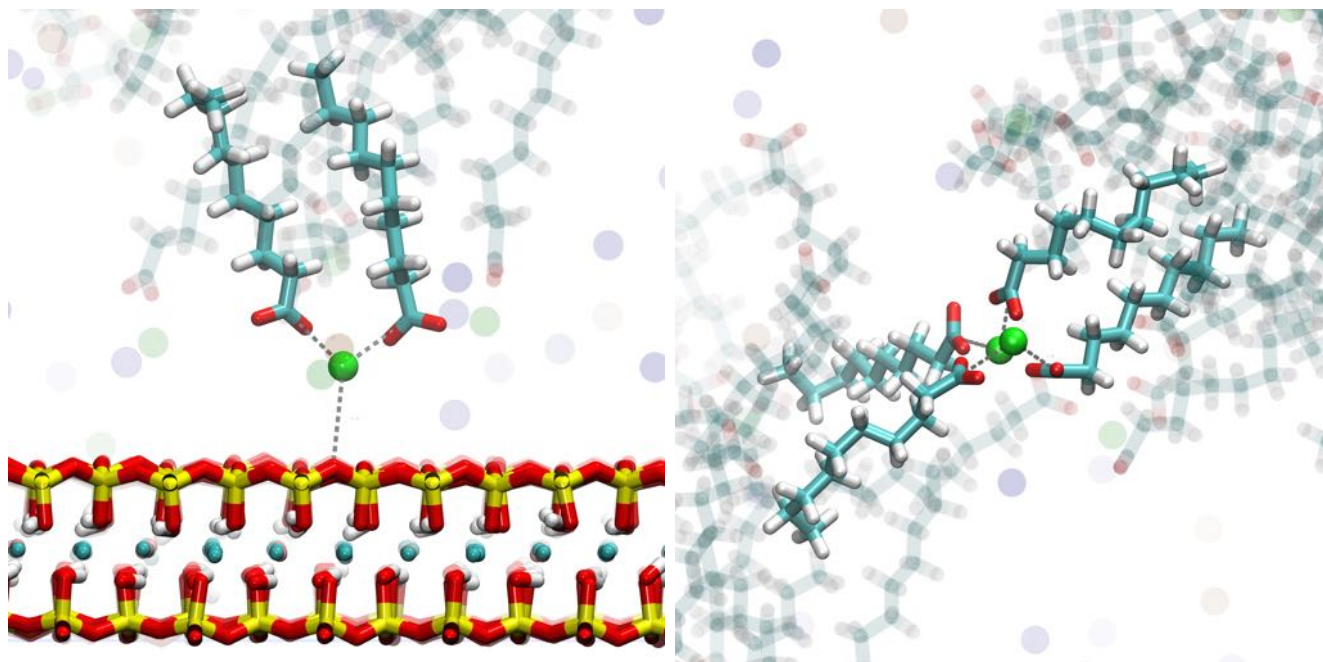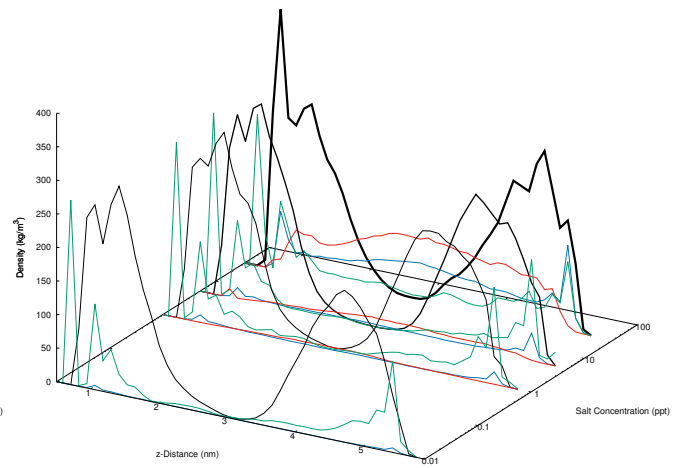

(a) Cation-charged bridging between clay and charged Na-decanoate molecules.

(b) Cation-charged bridging between identical organic molecules.
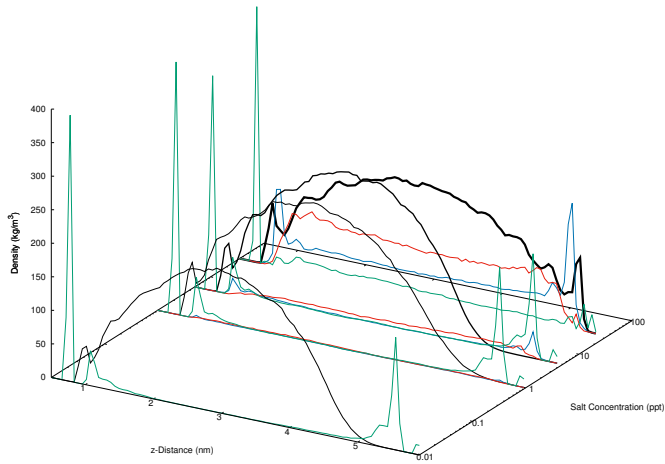
Figure 9: Enhanced snapshots of Na-decanoate interacting with CaMMT, Figure 8b. Colors as defined in section 2.5.
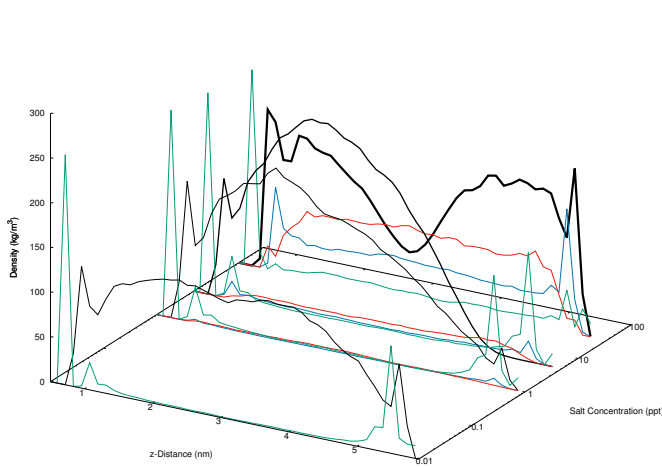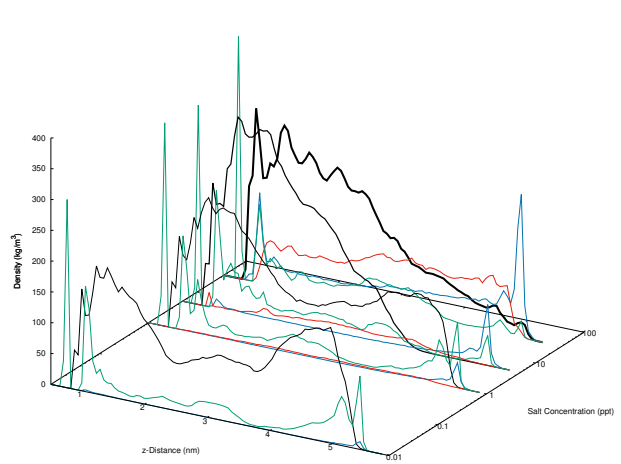
(a) CaMMT interacting with decanoic acid. Averaged between 5 ns and 10 ns.
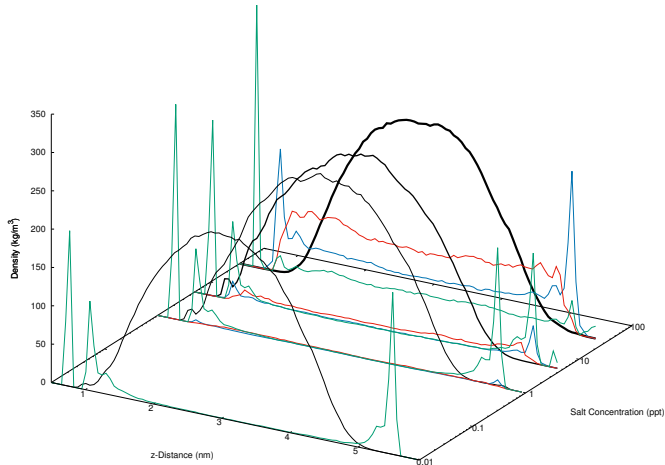
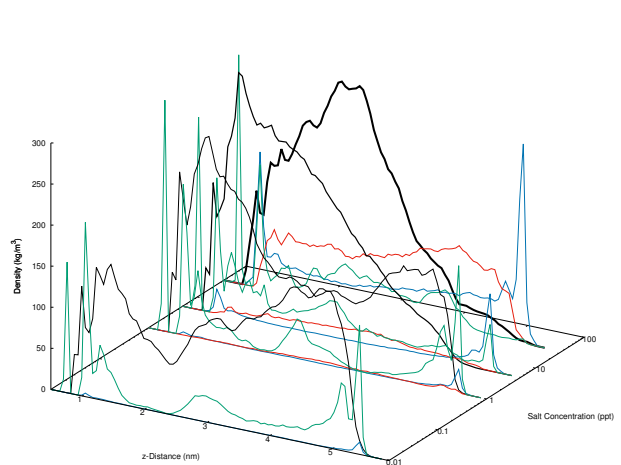(b) CaMMT interacting with Na-decanoate. Averaged between 5 ns and 10 ns.

(c) CaMMT interacting with decanoic acid. Averaged between 15 ns and 20 ns.

(d) CaMMT interacting with Na-decanoate. Averaged between 45 ns and 50 ns.

(e) CaMMT interacting with decanoic acid. Averaged between 45 ns and 50 ns.

(f) CaMMT interacting with Na-decanoate. Averaged between 95 ns and 100 ns.

Figure 11: Density profiles of initially oil-wet CaMMT interacting with decanoic acid (left) and Na-decanoate (right) at various salinities averaged over various times of the same production run. Colors as defined in section 2.5.
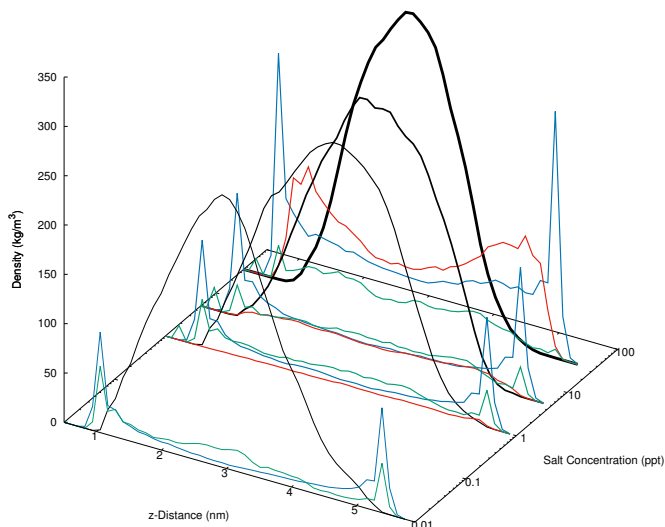
Figure 10: The density profile of CaMMT interacting with 80 Na-decanoate molecules at various salinities. Colors as defined in section 2.5.

3.5 Oil-wet vs. water-wet clays

To examine the difference between initially water-wet and initially oil-wet clay basal planes, the corresponding oil-wet systems were created as described in Section 2.1. The following results are taken from the last 5 ns of a 10 ns production run.

Initially oil-wet simulations of organics interacting with NaMMT resulted in the formation of organic aggregates between clay layers at all salinities. Initially oil-wet clays behaved identically to water-wet clays in the absence of divalent cations (see supplementary information).

Initially oil-wet simulations of decane interacting with CaMMT resulted in the formation of organic aggregates between the clay layers at all salinities, showing that non-polar uncharged organic molecules do not contribute to the wettability of a clay surface.

Figures 11a and 11b presents the density profiles of decanoic acid and Na-decanoate between CaMMT clay layers at various salinity levels.

Figure 11a presents the density profiles of decanoic acid molecules and ions between initially oil-wet CaMMT layers. Note the widely varying density profiles of organic molecules as a function brine concentration. The fresh water system creates an almost homogenous distribution of organics, whilst the calcium ions shield the charge of the clay. As the brine strength

is increased to 1‰ and 5‰ NaCl respectively, the formation of organic aggregates on the clay surface is seen.

Figure 11b presents the density profile of Na-decanoate interacting with CaMMT at various salt concentrations. The presence of charged organics and divalent cations maintain the oil-wet state of the system irrelevant of the salt concentration. This highlights that the protonation of the acids in the oil, and hence the pH level surrounding the clay, plays a vital role in low-salinity EOR.

3.6 Extended simulations initially oil-wet CaMMT

The large discrepancy in density profiles of oil-wet and water-wet charged organics interacting with CaMMT suggested extended simulations were warranted.

Figures 11c and 11e present the density profiles of polar decanoic acid averaged between 15 ns and 20 ns, and 45 ns and 50 ns of the same production run respectively. The results show that extending the simulation of decanoic acid interacting with initially oil-wet CaMMT to 50 ns reproduced organic aggregates between clay layers. The final state of polar decanoic acid interacting with CaMMT is independent of salinity, however the dynamics of polar organic desorption appear to be salt dependent (see the following sections 3.7 and 3.8).

Figures 11d and 11f present the density profiles of charged decanoate averaged between 45 ns and 50 ns, and 95 ns and 100 ns of the same production run. Both figures show desorption of organics from one basal plane as divalent cations are replaced by monovalent cations. Again, it is concluded that the replacement of divalent for monovalent cations and hence the ionic content of a flood is more important than its salinity.

To summarise, all initially oil-wet simulations of NaMMT show desorption of organic matter from the clay surface. Hence, replacing all the divalent cations in the system with monovalent cations will increase EOR effects.

Negatively charged decanoate molecules will remain adsorbed to a clay surface when a bridg-

ing cation is present via the cation-charged bridging mechanism. This effect is independent of salt concentration.

The results concord with the hypothesis that the initial wetness of the reservoir matrix is of importance to EOR,[3] but also propose that that the wettability of a reservoir is directly affected by its ionic content. Initially oil-wet NaMMT becomes water-wet independent of the organic molecule and salt concentration, whilst initially oil-wet CaMMT may remain oil-wet depending upon the organics constituting the oil. Further, the results suggests that the ionic content of a water-flood may be more important that its salinity, flooding a field with monovalent ions will increase the wettability of the reservoir matrix.

3.7 Dynamic clustering analysis

Clustering of organic molecules is observed in all simulations to some extent. Clustering analysis over a simulations trajectory probes the dynamic effects of this process.

Figure 12a shows the number of clusters in the simulation of decanoic acid interacting with initially water-wet NaMMT as a function of time and salt concentration. It can be seen that the formation of micelles occurs on the nanoscale independently of salinity. The noise at approximately 6 and 8 ns corresponds to a single molecule breaking off of the dominant cluster and instantaneously being reabsorbed into the micelle.

The behaviour presented in Figure 12a is typical amongst all the initially water-wet simulations of both NaMMT and CaMMT with all three forms of organics.

Figure 12b presents the number of organic clusters for initially water-wet NaMMT interacting with Na-decanoate. In this system, the organics form several separate clusters, rather than one large aggregate, as is the case of Na-decanoate interacting with CaMMT (supplementary information). This is because the charged decanoate molecules repel each other, whilst in the water-wet CaMMT system, the divalent cations can bridge the like-charged organics to one another.

Figure 12c presents the number of clusters of polar decanoic acid interacting with initially oil-wet NaMMT as a function of time and salt concentration. The initial number of clusters in this simulation is two, i.e. one cluster on each of the modelled clay surfaces. As the simulations progress, several organic molecules break away from the oil-wet surface to create a new separate cluster. This process continues, and within 1 ns the maximum number of separate clusters can be seen. After a nanosecond, the separate clusters begin to coalesce, and any further organics desorbed from the clay surface are rapidly encompassed in one of the previously existing clusters.

The only scenario where this behaviour is not observed is for originally oil-wet simulations of CaMMT interacting with charged decanoate, Figure 12d. These systems remain oil-wet as previously discussed, and the number of clusters does not vary over the timescale modelled.

## 3.8 Dynamic divalent cation bridge analysis

A divalent cation bridge is determined to be any divalent cation that is within 5 Å of the clay surface and within 3 Å of an organic oil molecule, as discussed in analysis techniques, section 2.4. This measure is a useful quantity in determining the rate of organic desorption from a clay surface, and is useful to determine both the occurrence of divalent cation bridging as well as its dependence on salt concentration.

Figure 13a presents the number of divalent cation-polar bridges for the initially oil-wet simulation of CaMMT interacting with polar decanoic acid. Here, the number of cation bridges decreases as the simulation progresses, and that the difference between salinity levels is minimal. At the end of all simulations the number of potentially cation bridging cations has reduced to near zero.

Figure 13b presents the number of divalent cation-charged bridges for initially oil-wet simulations of CaMMT interacting with charged Na-decanoates at various salt concentrations. Note, the increased amount of bridges in this system compared to the polar decanoic acid,
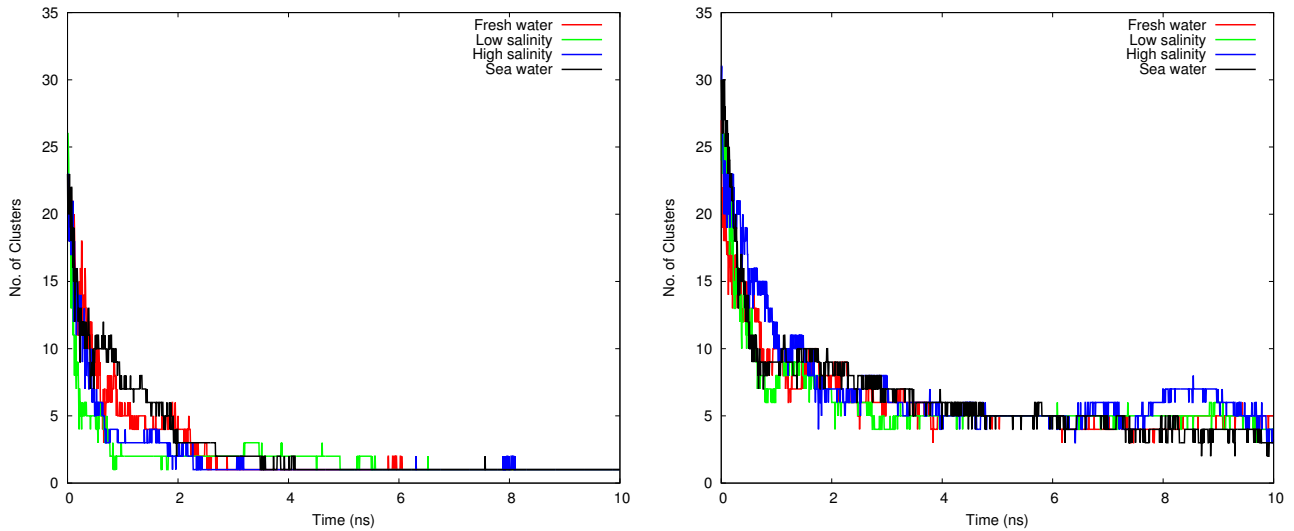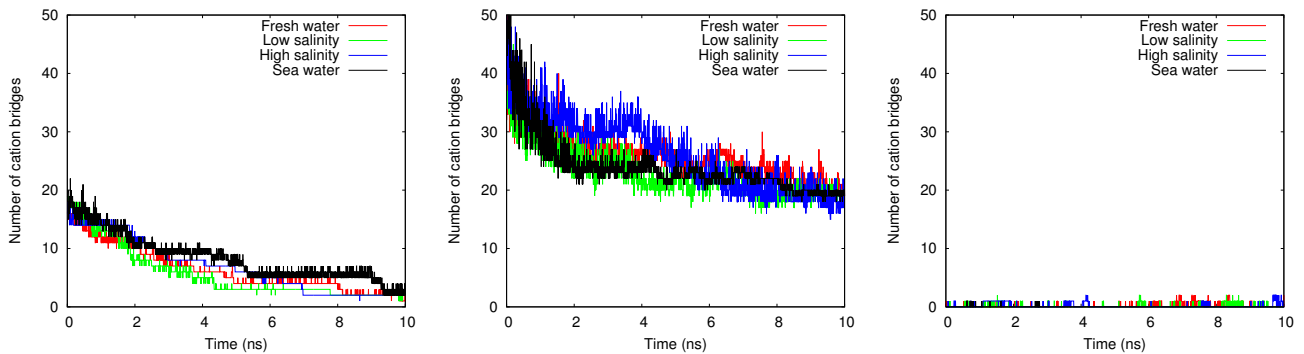
(a) Initially water-wet NaMMT with decanoic acid. (b) Initially water-wet NaMMT with Na-decanoate.
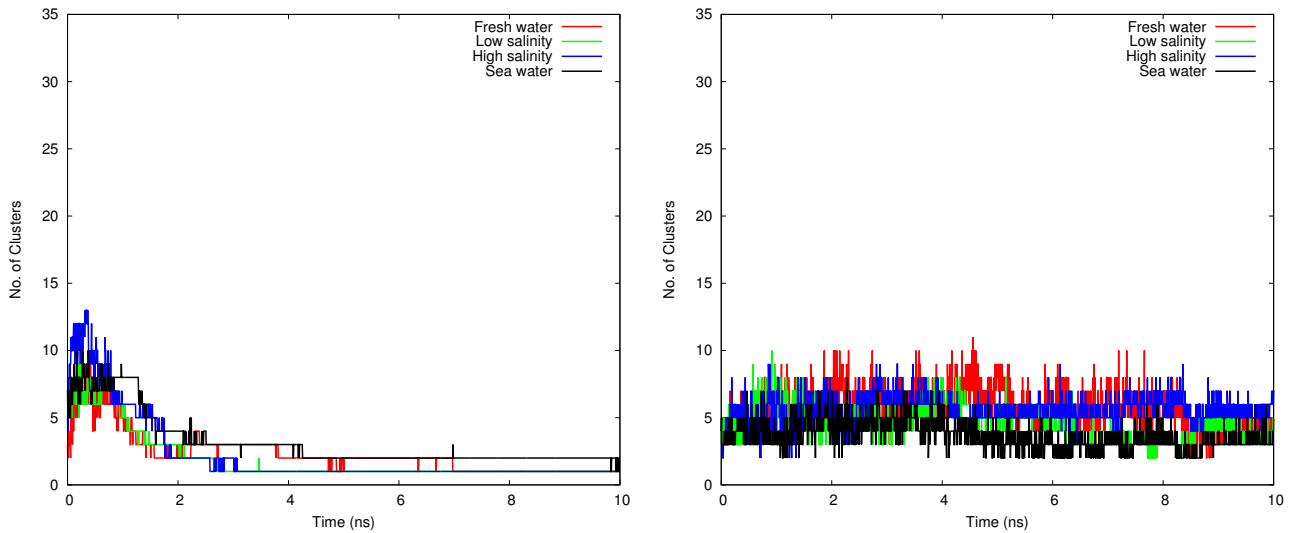
(c) Initially oil-wet NaMMT with decanoic acid. (d) Initially oil-wet CaMMT with Na-decanoate.

Figure 12: The number of cluster of a simulation as a function of time and salt concentration. See legends for color scheme.

(a) Initially oil-wet CaMMT with decanoic acid.

(b) Initially oil-wet CaMMT with Na-Decanoiate.

(c) Initially water-wet CaMMT with Na-Decanoate.

Figure 13: The rate of change of potentially bridging divalent cations as a function of time and salt concentration. See legends for color scheme.

this is due to the charge of the organic. There is a slight decrease in the total number of bridges with time, however the number of cation-charged bridges appears to converge to a non-zero number during the simulation. Also note the independence of salinity in cation-charged bridging.

In general, all systems of CaMMT present a decrease of divalent cation bridges with time, and all are independent of interlayer salinity. The amount of cation bridges in simulations of oil wet CaMMT with decane decreases to zero after 1 ns, decreases to zero after 10 ns for decanoic acid, and converges to a finite number with decanoate.

Figure 13c shows the number of divalent cation bridges for initially water-wet CaMMT interacting with Na-decanoate. It can be seen that there are intermittent cation-charged bridging events occurring throughout the simulation, however these events flitter in and out of existence. The initial wettability of a clay appears to be an important factor for the cation-charged bridging mechanism, as previously discussed.

4   Conclusions

The use of molecular dynamics simulations have helped elucidate some of the key mechanism underpinning low-salinity enhanced oil recovery. The following are the key conclusions discerned from the simulations of smectite clays with oil organics as a function of salinity and initial clay wetness.

Electric double layer expansion does not vary with salinity, and is not a driving factor for low-salinity EOR. Further work is required to interpret the importance of pH on the effective charge of the clay basal plane.

All multicomponent ionic exchange mechanisms proposed to affect low-salinity EOR, figure 2, are *independent of salt concentration* and hence cannot explain the effects of low-salinity EOR. Non-polar, uncharged organic molecules do not interact with charged hydrated smectite clay minerals to any extent. Polar, uncharged molecules form micelles, and do not interact with charged smectite clay surfaces profusely. Depending upon a clay's initial wettability, charged organic molecules can interact heavily with clay basal planes. For an initially oil-wet clay, the cation bridging mechanism is prevalent, whilst for an initially water-wet clay, the cation bridging mechanism is absent. Water bridging has not been observed in any simulation, however more densely charged divalent cations, i.e. Mg^{2+}, may be required to observe such effects. A Stern layer of unhydrated calcium cations is observed in both oil-wet and water-wet simulations of CaMMT. The amount of unhydrated cations in the Stern layer is independent of the salt concentration of the system, and hence divalent cation bridging and ligand bridging may occur independently of salt concentration.

The simulations present that, in the systems studied, the key drivers of low-salinity EOR are twofold.

One, the pH level surrounding the clay, and hence the protonation and charge of organic oil molecules. Cation-charged bridging is present between oil-wet clay and organic, however divalent cation-polar bridging is not. A key question arises in how the salt concentration surrounding the clay surface might affect the protonation of the polar acids within oil? Investigation of this mechanism would require QM modelling.

Two, that the wettability of a clay is dependent upon the charge balancing cation. The simulations show that by replacing divalent calcium ions with monovalent sodium cations will increase clay water wetness, and improve oil recovery rates. The ionic content of a flood is more important that the concentration.

The molecular level insight into clay organic interactions occurring during EOR offer hitherto unaccessed resolution. Future work shall investigate the role of $CaCl_2$ as well as NaCl brine to further elucidate the effect of monovalent vs divalent cations on the wetness of clays. Highly hydrating cations, such as Mg^{2+} may also be modelled to examine the full potential of water bridging in EOR. The cation exchange mechanism shall be investigated by modelling positively charged organics (containing nitro-

gen in the functional group) and organics containing aromatic rings. This shall determine whether cation-π interactions play any role in low-salinity EOR. Further clay minerals found at a higher abundance within reservoirs, such as kaolinite and illite, shall also be modelled.

Supporting Information Available: Radial distribution functions have been used to determine cut-offs for cation bridging events, these can be viewed on-line. Density profiles, dynamic clustering and dynamic cation bridging figures are also available on-line: This material is available free of charge via the Internet at `http://pubs.acs.org/`.

References

(1) *World Energy Outlook 2013*; International Energy Agency, Organization for Economic Co-operation and Development, 2013.

(2) Sheng, J. *Modern Chemical Enhanced Oil Recovery: Theory and Practice*; Gulf Professional Publishing, 2010.

(3) Sharma, M.; Filoco, P. Effect of brine salinity and crude-oil properties on oil recovery and residual saturations. *SPE J. (Soc. Pet. Eng.)* **2000**, *5*, 293–300.

(4) Tang, G.-Q.; Morrow, N. R. Influence of brine composition and fines migration on crude oil/brine/rock interactions and oil recovery. *J. Pet. Sci. Eng.* **1999**, *24*, 99–111.

(5) Zhang, Y.; Morrow, N. R. Comparison of secondary and tertiary recovery with change in injection brine composition for crude-oil/sandstone combinations. SPE/DOE Symposium on Improved Oil Recovery. 2006.

(6) Mohan, K. K.; Vaidya, R. N.; Reed, M. G.; Fogler, H. S. Water sensitivity of sandstones containing swelling and non-swelling clays. *Colloids Surf., A* **1993**, *73*, 237–254.

(7) Skrettingland, K.; Holt, T.; Tweheyo, M. T.; Skjevrak, I. Snorre low-salinity-water injection - Core flooding experiments and single-well field pilot. *SPE Reservoir Eval. Eng.* **2011**, *14*, 182–192.

(8) Austad, T.; Rezaei-Doust, A.; Puntervold, T. Chemical mechanism of low salinity water flooding in sandstone reservoirs. Proceedings of the 2010 Society of Petroleum Engineers (SPE) Improved Oil Recovery Symposium. 2010; pp 24–28.

(9) Fassi-Fihri, O.; Robin, M.; Rosenberg, E. Wettability studies at the pore level: a new approach by the use of cryo-scanning electron microscopy. *SPE Form. Eval.* **1995**, *10*, 11–19.

(10) Civan, F. *Reservoir Formation Damage*; Gulf Professional Publishing, 2011.

(11) Bantignies, J.-L.; Moulin, C. C. D.; Dexpert, H. Wettability contrasts in kaolinite and illite clays: characterization by infrared and X-ray absorption spectroscopies. *J. Phys. IV* **1997**, *7*, C2–867.

(12) Sheng, J. Critical review of low-salinity waterflooding. *J. Pet. Sci. Eng.* **2014**, *120*, 216–224.

(13) Verwey, E. J. W.; Overbeek, J. T. G.; Overbeek, J. T. G. *Theory of the Stability of Lyophobic Colloids*; Courier Dover Publications, 1999.

(14) Lager, A.; Webb, K.; Black, C.; Singleton, M.; Sorbie, K. Low salinity oil recovery - An experimental investigation. *Petrophysics* **2008**, *49*, 28.

(15) Sposito, G. *The Chemistry of Soils*; Oxford university press, 2008.

(16) McGuire, P.; Chatham, J.; Paskvan, F.; Sommer, D.; Carini, F. Low salinity oil recovery: an exciting new EOR opportunity for Alaska's North Slope. SPE Western Regional Meeting. 2005.

(17) Geatches, D. L.; Jacquet, A.; Clark, S. J.; Greenwell, H. C. Monomer adsorption on kaolinite: modeling the essential ingredients. *J. Phys. Chem. C* **2012**, *116*, 22365–22374.

(18) Zhong, J.; Wang, X.; Du, J.; Wang, L.; Yan, Y.; Zhang, J. Combined molecular dynamics and quantum mechanics study of oil droplet adsorption on different self-assembly monolayers in aqueous solution. *J. Phys. Chem. C* **2013**, *117*, 12510–12519.

(19) Sánchez, V. M.; Miranda, C. R. Modeling acid oil component Interactions with carbonate reservoirs: a first-principles view on low salinity recovery mechanisms. *J. Phys. Chem. C* **2014**, *118*, 19180–19187.

(20) Suter, J. L.; Anderson, R. L.; Greenwell, H. C.; Coveney, P. V. Recent advances in large-scale atomistic and coarse-grained molecular dynamics simulation of clay minerals. *J. Mater. Chem.* **2009**, *19*, 2482–2493.

(21) Greenwell, H. C.; Jones, W.; Coveney, P. V.; Stackhouse, S. On the application of computer simulation techniques to anionic and cationic clays: A materials chemistry perspective. *J. Mater. Chem.* **2006**, *16*, 708–723.

(22) Van Duin, A. C.; Dasgupta, S.; Lorant, F.; Goddard, W. A. ReaxFF: a reactive force field for hydrocarbons. *J. Phys. Chem. A* **2001**, *105*, 9396–9409.

(23) Downs, R. T.; Hall-Wallace, M. The American Mineralogist crystal structure database. *Am. Mineral.* **2003**, *88*, 247–250.

(24) Liu, X.; Lu, X.; Sprik, M.; Cheng, J.; Meijer, E. J.; Wang, R. Acidity of edge surface sites of montmorillonite and kaolinite. *Geochim. Cosmochim. Acta* **2013**, *117*, 180–190.

(25) Tazi, S.; Rotenberg, B.; Salanne, M.; Sprik, M.; Sulpizi, M. Absolute acidity of clay edge sites from ab-initio simulations. *Geochim. Cosmochim. Acta* **2012**, *94*, 1–11.

(26) Hanwell, M. D.; Curtis, D. E.; Lonie, D. C.; Vandermeersch, T.; Zurek, E.; Hutchison, G. R. Avogadro: An advanced semantic chemical editor, visualization, and analysis platform. *J. Cheminf.* **2012**, *4*, 17.

(27) Barratt, M. Quantitative structure-activity relationships (QSARs) for skin corrosivity of organic acids, bases and phenols: principal components and neural network analysis of extended datasets. *Toxicol. In Vitro* **1996**, *10*, 85–94.

(28) Cygan, R. T.; Liang, J.-J.; Kalinichev, A. G. Molecular models of hydroxide, oxyhydroxide, and clay phases and the development of a general force field. *J. Phys. Chem. B* **2004**, *108*, 1255–1266.

(29) Vanommeslaeghe, K. et al. CHARMM general force field: A force field for drug-like molecules compatible with the CHARMM all-atom additive biological force fields. *J. Comput. Chem.* **2010**, *31*, 671–690.

(30) Bjelkmar, P.; Larsson, P.; Cuendet, M. A.; Hess, B.; Lindahl, E. Implementation of the CHARMM force field in GROMACS: analysis of protein stability effects from correction maps, virtual interaction sites, and water models. *J. Chem. Theory Comput.* **2010**, *6*, 459–466.

(31) Wright, L. B.; Walsh, T. R. First-principles molecular dynamics simulations of NH4+ and CH3COO- adsorption at the

aqueous quartz interface. *J. Chem. Phys.* **2012**, *137*, 224702.

(32) Hess, B.; Kutzner, C.; van der Spoel, D.; Lindahl, E. GROMACS 4:âĂĽ Algorithms for highly efficient, load-balanced, and scalable molecular simulation. *J. Chem. Theory Comput.* **2008**, *4*, 435–447.

(33) Franks, F. *Water: A Matrix of Life*; RSC paperbacks; Royal Society of Chemistry, 2000.

(34) Humphrey, W.; Dalke, A.; Schulten, K. VMD: Visual molecular dynamics. *J. Mol. Graphics* **1996**, *14*, 33–38.

(35) Bourg, I. C.; Sposito, G. Molecular dynamics simulations of the electrical double layer on smectite surfaces contacting concentrated mixed electrolyte (NaCl-CaCl2) solutions. *J. Colloid Interface Sci.* **2011**, *360*, 701–715.

(36) Tournassat, C.; Chapron, Y.; Leroy, P.; Bizi, M.; Boulahya, F. Comparison of molecular dynamics simulations with triple layer and modified Gouy-Chapman models in a 0.1 M NaCl-montmorillonite system. *J. Colloid Interface Sci.* **2009**, *339*, 533–541.

(37) Khelifa, A.; Stoffyn-Egli, P.; Hill, P. S.; Lee, K. Effects of salinity and clay type on oil-mineral aggregation. *Mar. Environ. Res.* **2005**, *59*, 235–254.

Graphical TOC Entry

The salt content of a water flood can dramatically alter the wettability of a reservoir matrix. Increasing monovalent sodium content, whilst decreasing divalent calcium content, has a marked effect on low-salinity EOR.